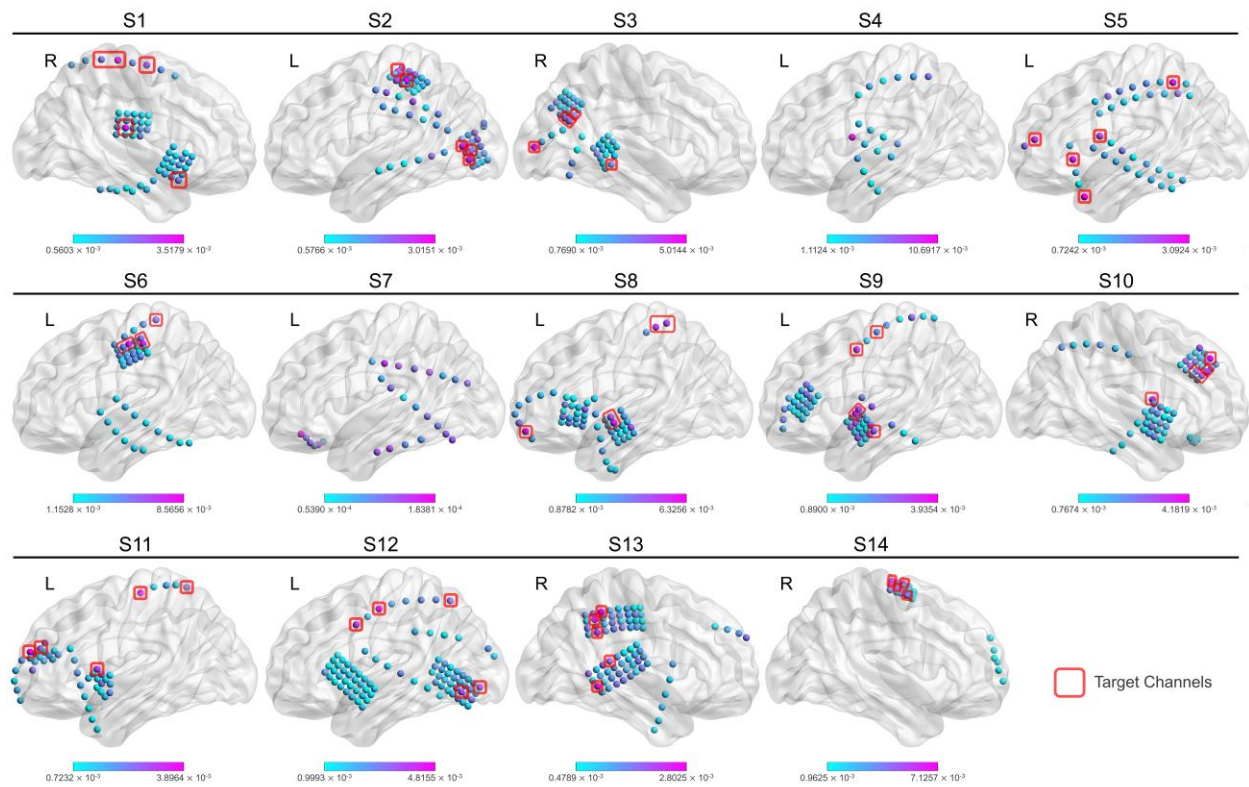


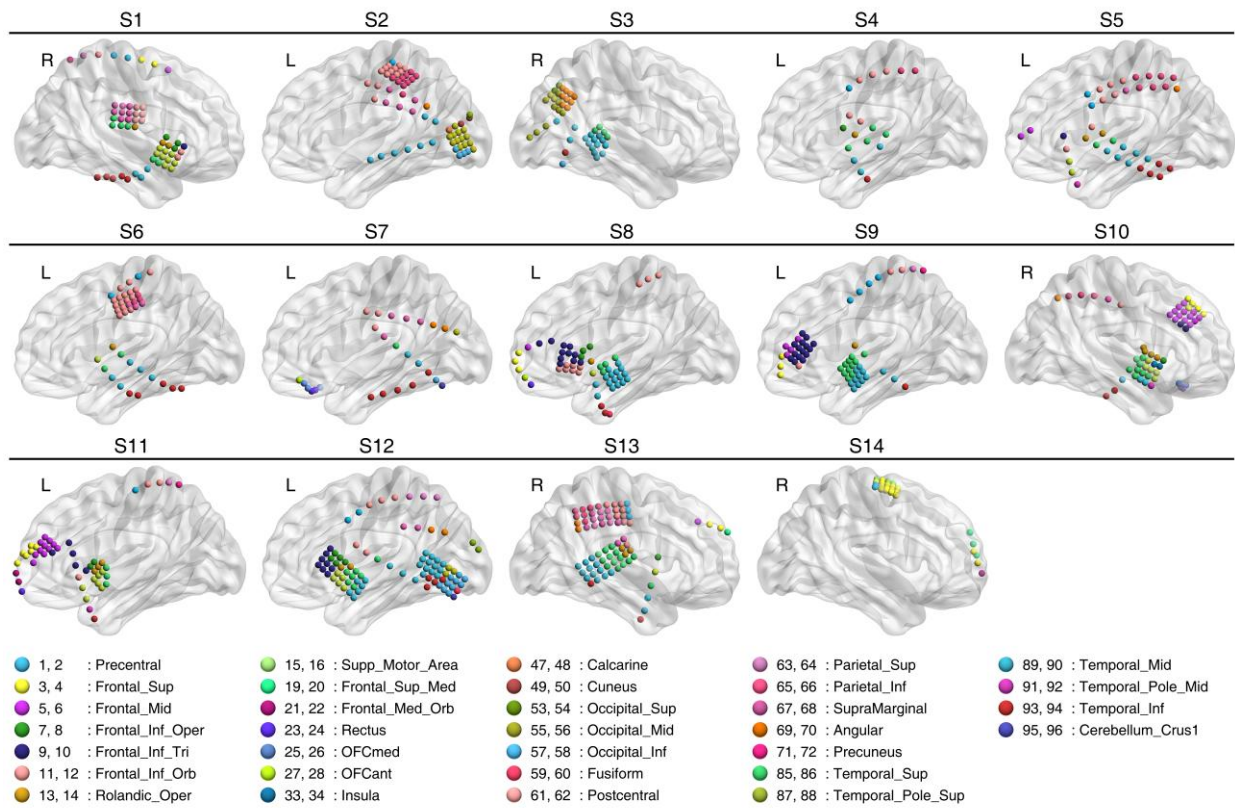
List of Supplementary Materials

- 1
- 2 **Supplementary Figure 1. Intra-subject XAI contribution maps.**
- 3 **Supplementary Figure 2. Electrode location across all subjects.**
- 4 **Supplementary Figure 3. Correlation coefficients of ground-truth signals with neurally-generated and**
- 5 **condition-channel signals.**
- 6 **Supplementary Figure 4. Intra-subject decoding results.**
- 7 **Supplementary Figure 5. Inter-subject XAI maps and elbow point-based channel selection.**
- 8 **Supplementary Figure 6. Spatial distribution of original and virtual electrodes.**
- 9 **Supplementary Figure 7. Inter-subject decoding results.**
- 10 **Supplementary Figure 8. Greater decoding performance improvement in subjects with lower baseline**
- 11 **performance.**
- 12 **Supplementary Figure 9. Inter-subject XAI contribution maps with generated virtual channels.**
- 13 **Supplementary Figure 10. Experimental setup for center-out reach-and-grasp task.**
- 14 **Supplementary Figure 11. Overview of the DDPM Framework.**
- 15 **Supplementary Table 1. Intra-subject analysis cases.**
- 16 **Supplementary Table 2. Inter-subject analysis channel configuration.**
- 17 **Supplementary Table 3. Demographic and clinical characteristics of the subjects.**
- 18 **Supplementary Table 4. Number of trials per session for each participant.**
- 19 **Supplementary Table 5. Model architecture of the Bi-LSTM decoder.**



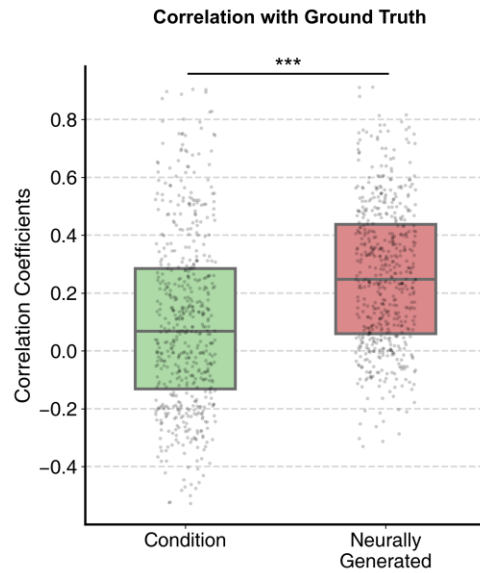
20

21 **Supplementary Figure 1. Intra-subject XAI contribution maps.** Integrated gradients were computed from
 22 subject-specific Bi-LSTM decoders trained on Session 1 data. Electrodes are color-coded by IG values, with higher
 23 values indicating greater contribution. The top five target channels used for intra-subject analysis are indicated,
 24 except for excluded subjects (S4 and S7). R, right lateral view; L, left lateral view.



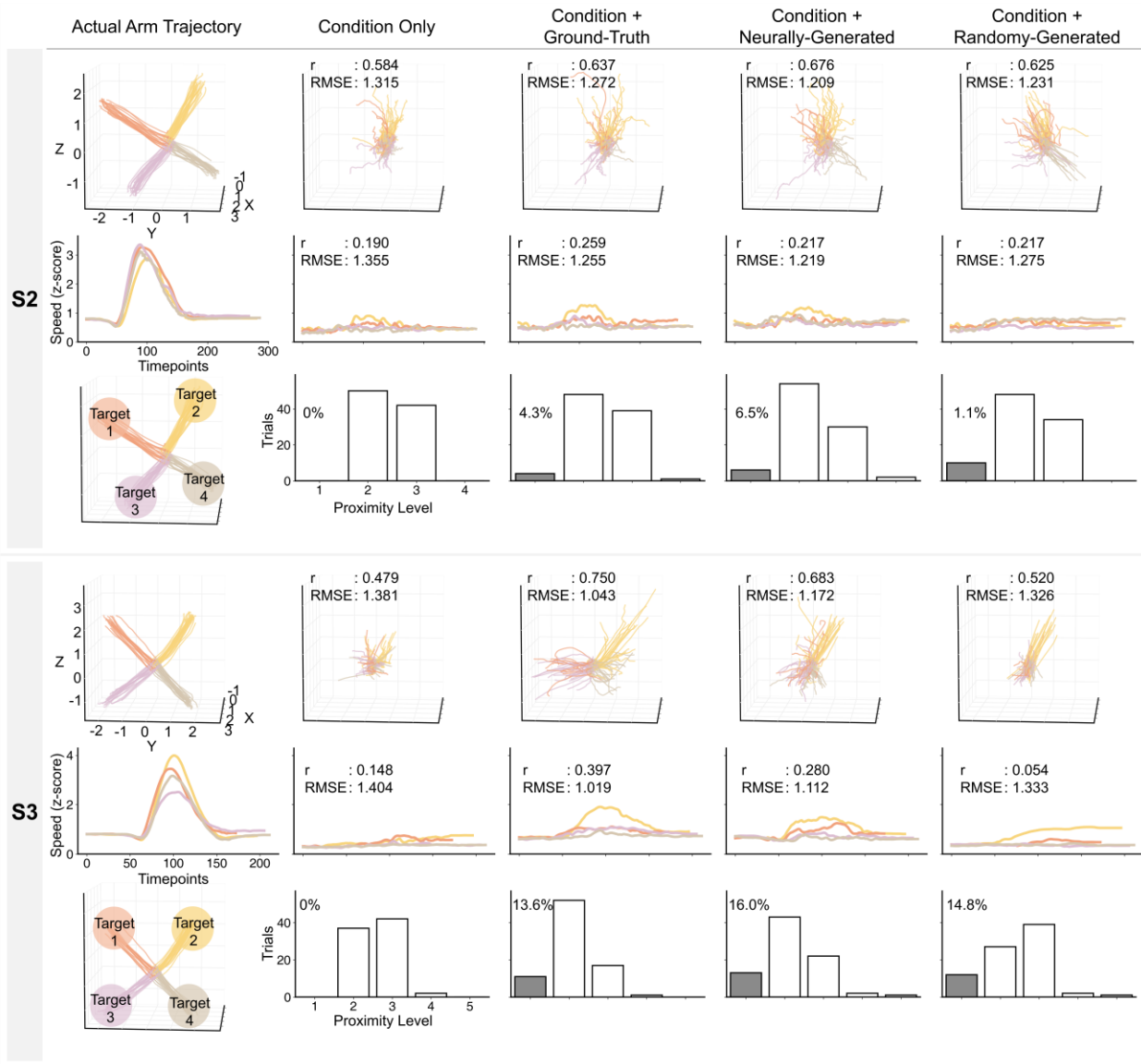
25

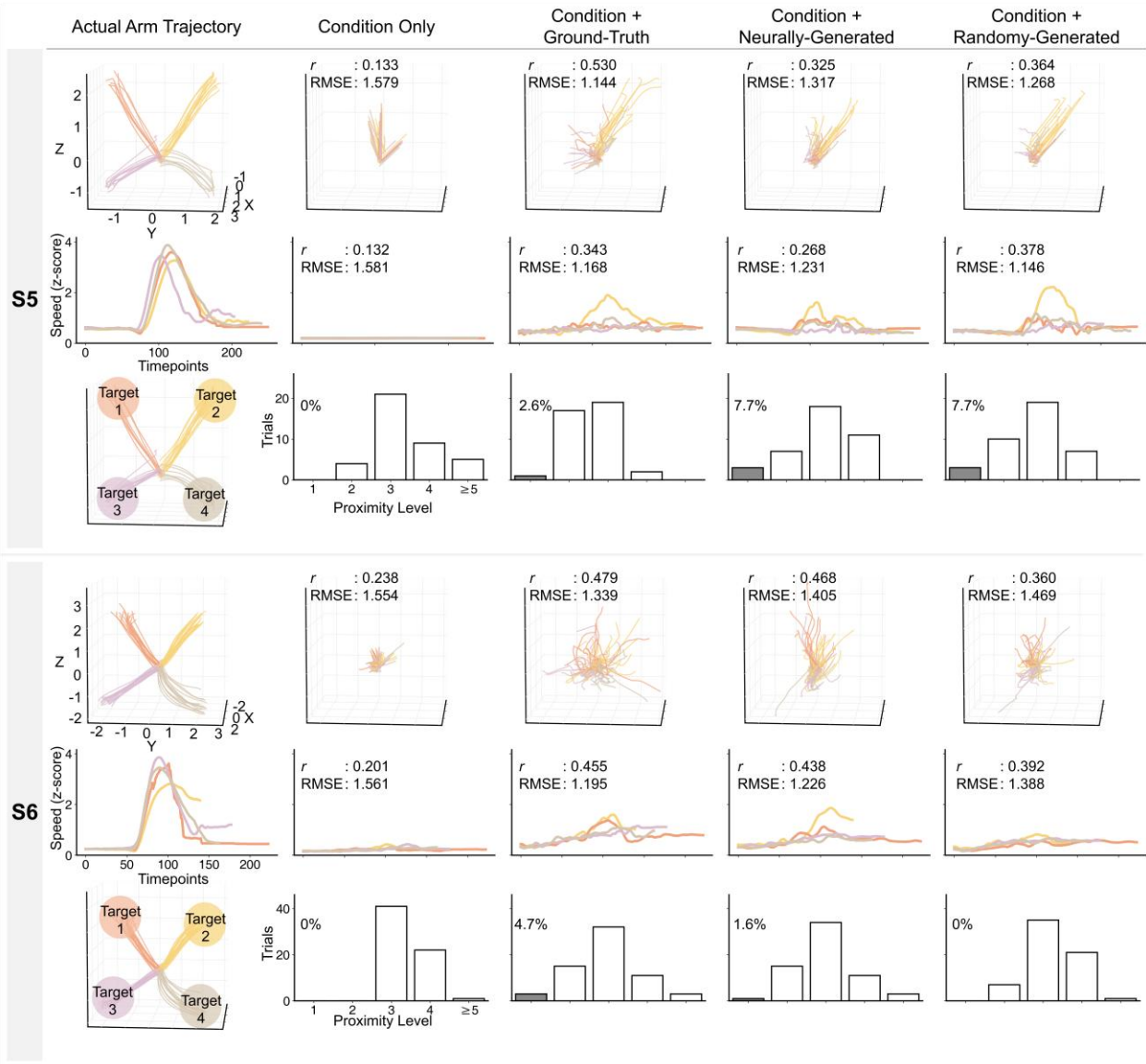
26 **Supplementary Figure 2. Electrode location across all subjects.** ECoG electrode locations projected onto an MNI
 27 template. Electrode placement was determined based on clinical requirements for seizure monitoring. Colors denote
 28 AAL3-defined region. Bad channels were excluded. R, right lateral view; L, left lateral view.

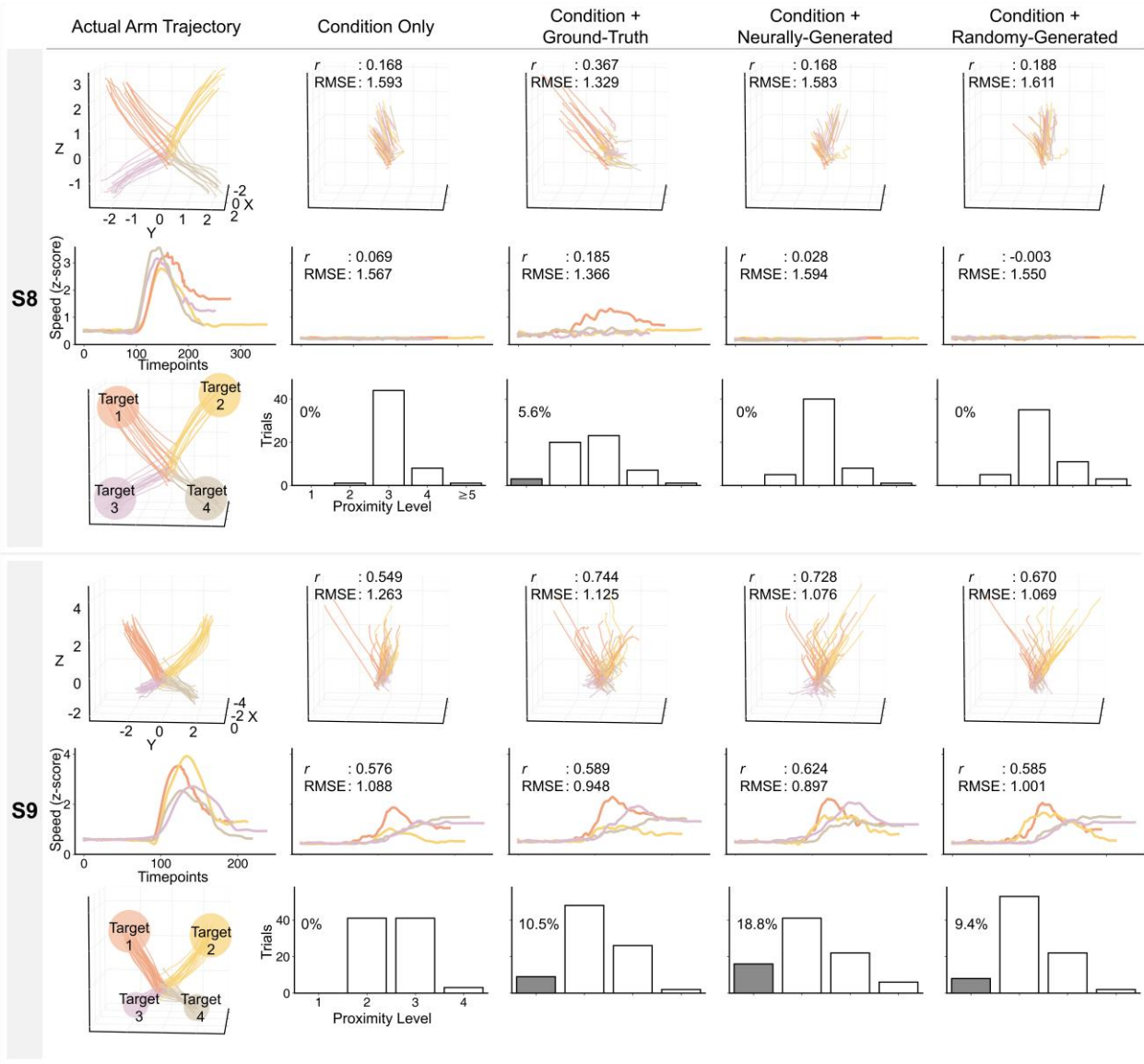


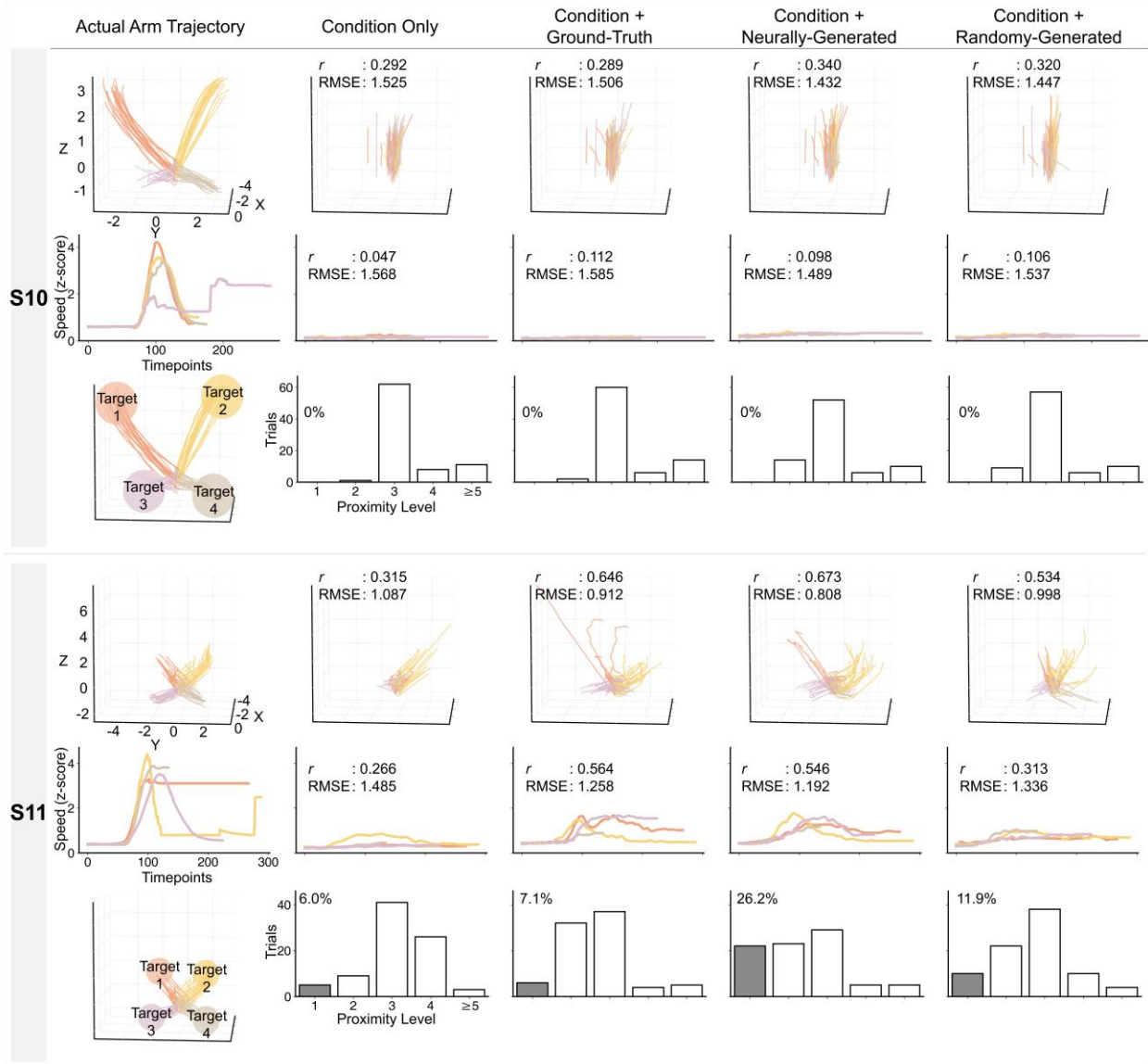
30

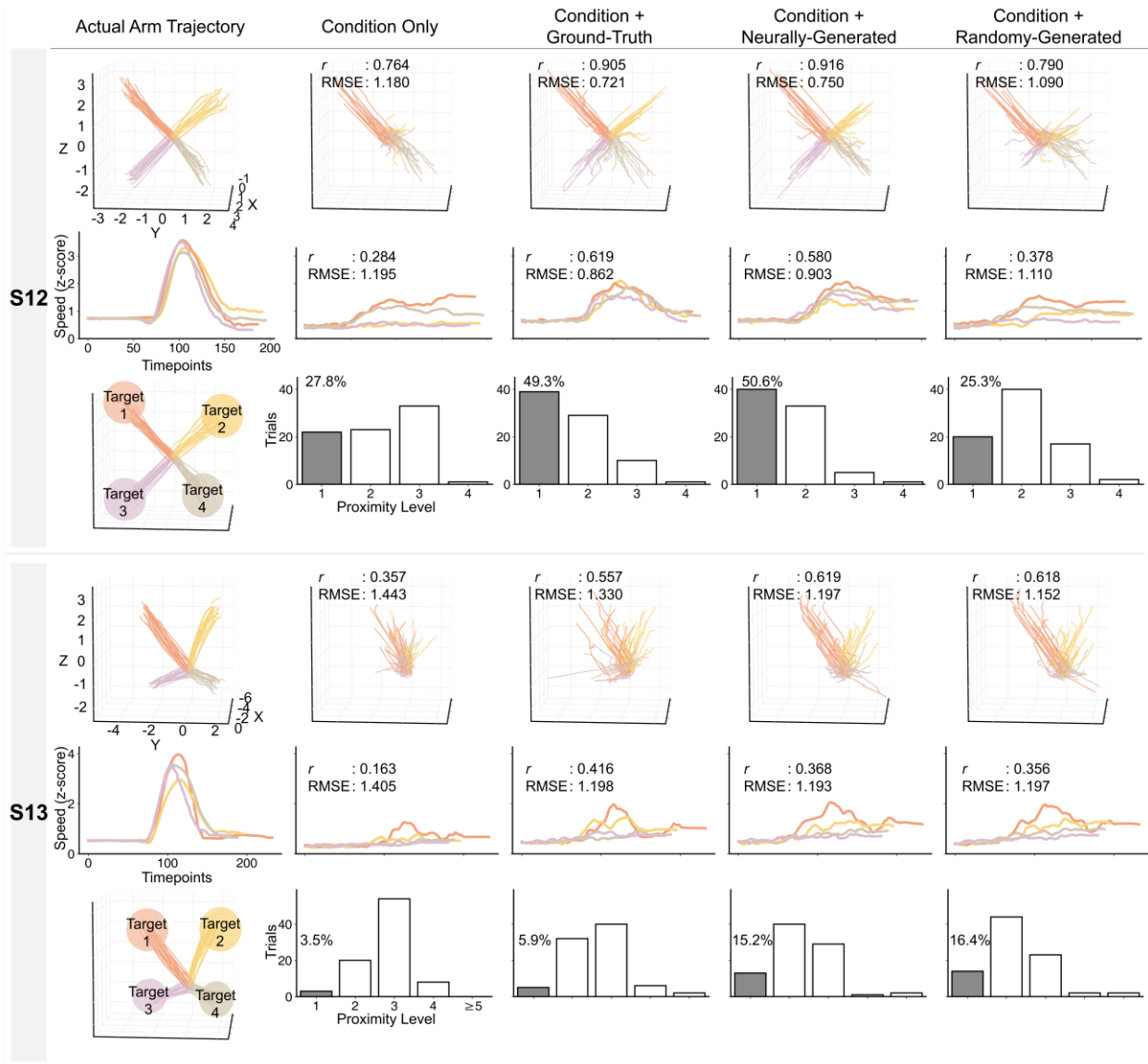
31 **Supplementary Figure 3. Correlation coefficients of ground-truth signals with neurally-generated and**
32 **condition-channel signals.** Correlation Coefficients between the ground truth and each signal type (condition
33 channel signals, and neurally-generated signals) across all cases ($n= 5$ target channels \times 110 cases = 550). For
34 condition channel signals, the maximum correlation coefficient across all target-condition pairs was used for each
35 case. Boxes represent the interquartile range (IQR; 25th-75th percentile) with the median indicated by the horizontal
36 line, and individual data points are shown as scatter dots. $*p < 0.05$, $**p < 0.01$, $***p < 0.001$; statistical
37 significance was assessed using two-sided pairwise Wilcoxon signed-rank tests.

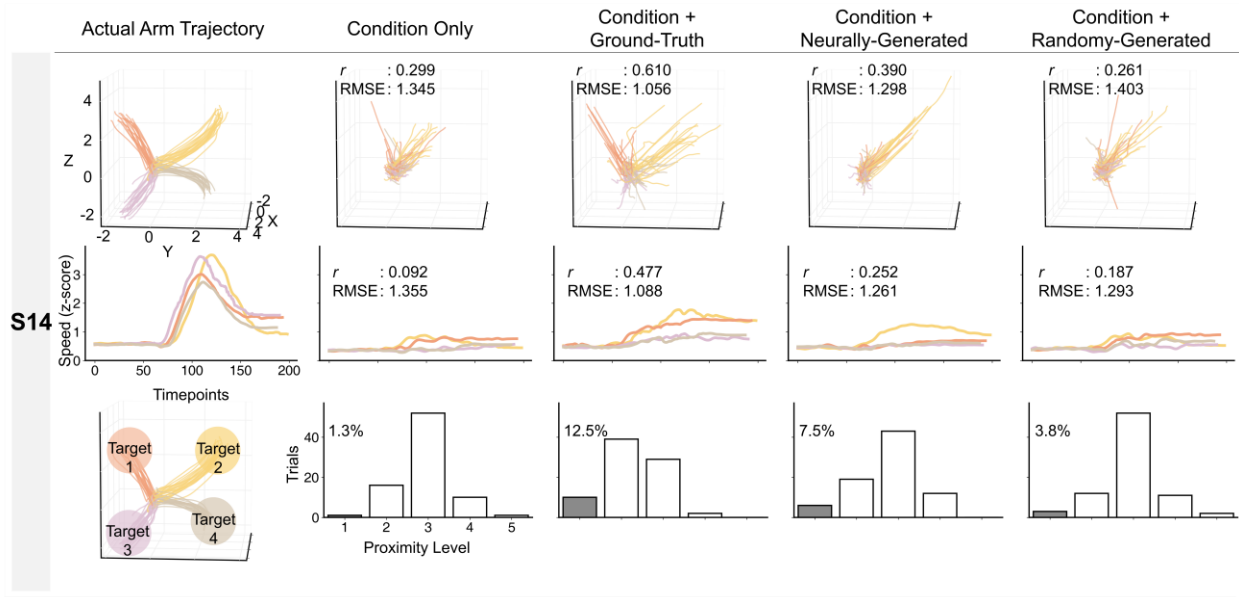






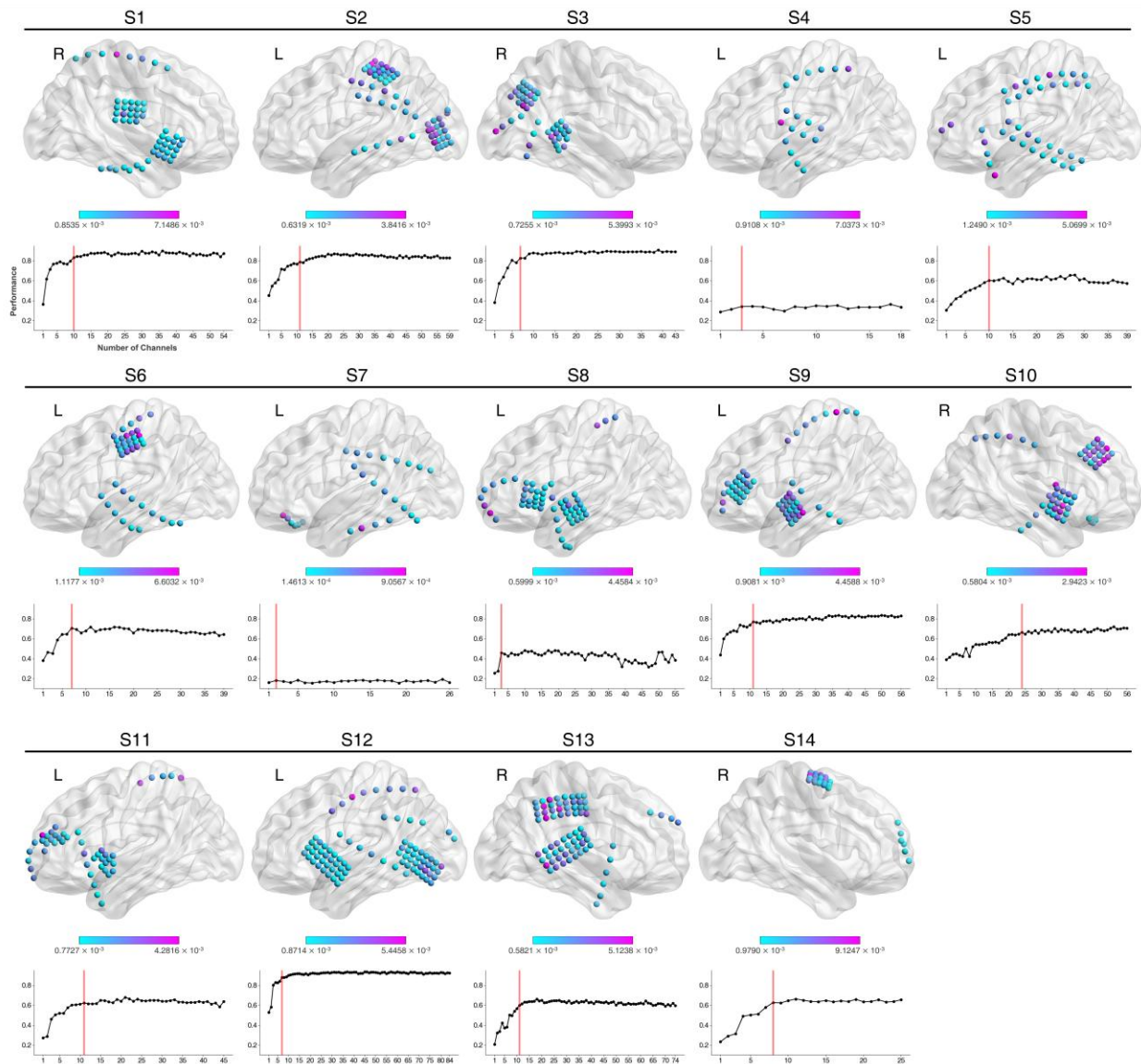






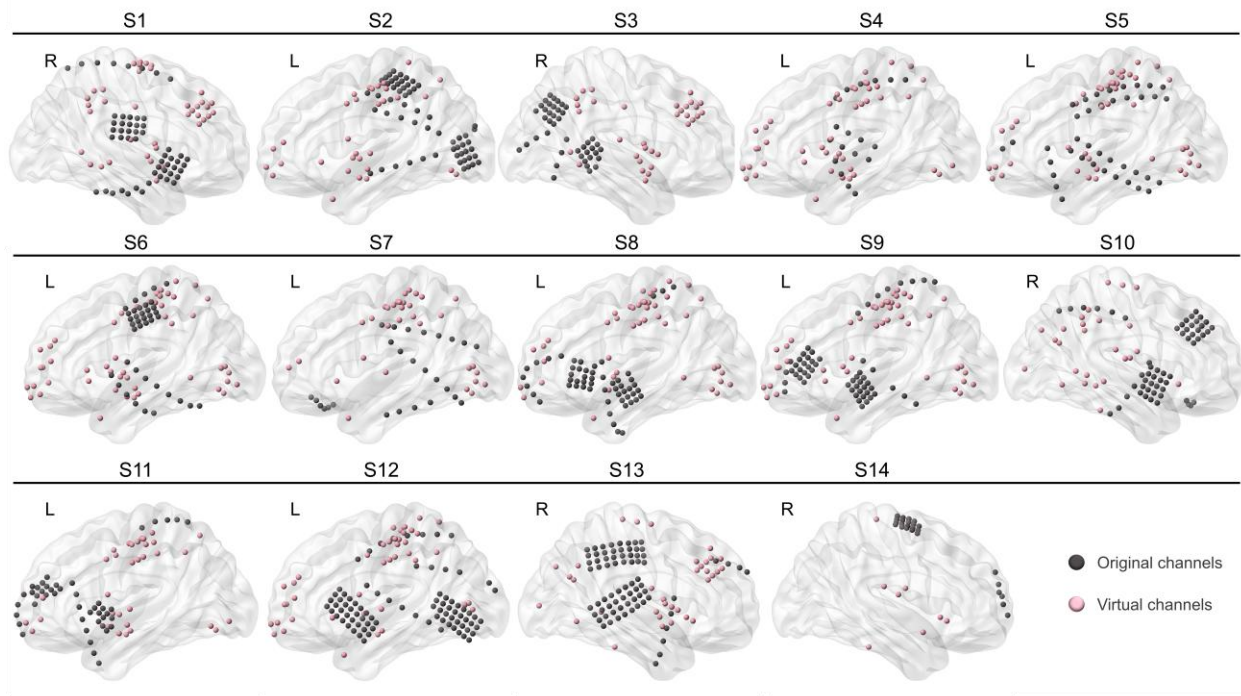
43

44 **Supplementary Figure 4. Intra-subject decoding results.** Representative intra-subject analysis results for
 45 individual subjects. Decoded trajectories, speed profiles, and endpoint reaching rate histograms are displayed,
 46 following the visualization format described in Figure 2.



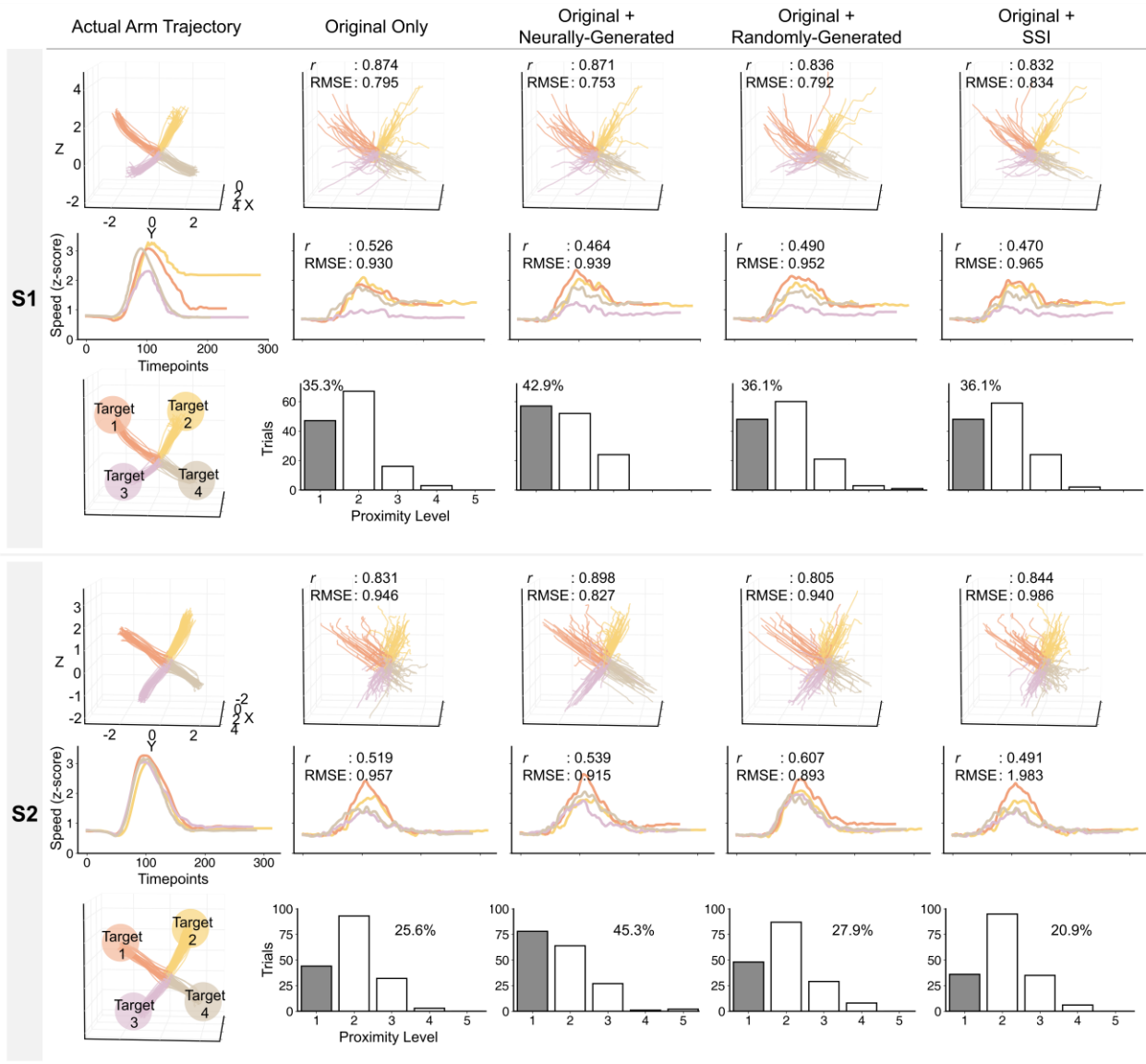
47

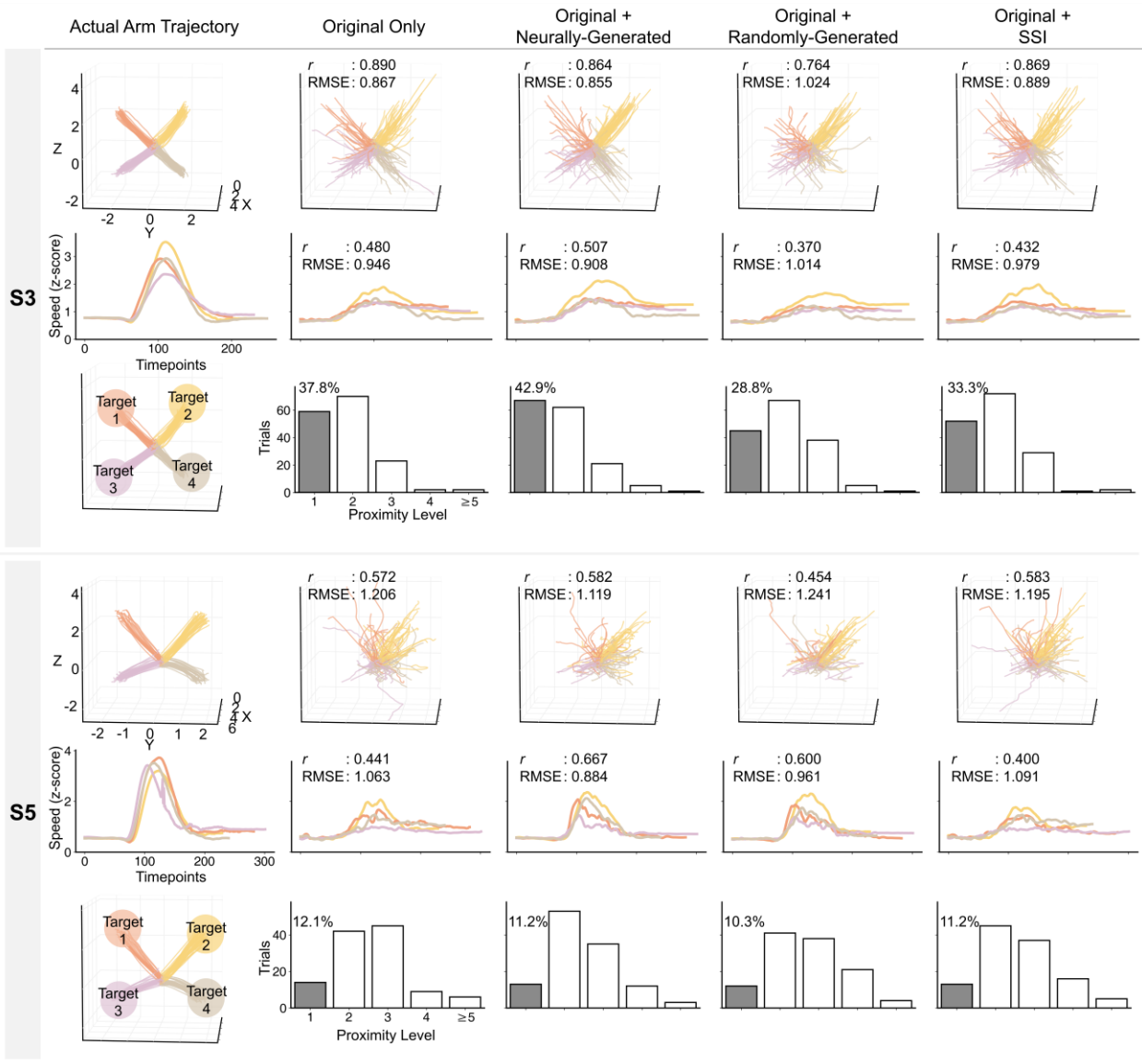
48 **Supplementary Figure 5. Inter-subject XAI maps and elbow point-based channel selection.** Inter-subject XAI
 49 contribution maps and the corresponding elbow point analysis for target channel selection, utilizing data from all
 50 sessions. For each subject, the contribution of all channels is mapped onto the cortical surface, followed by an
 51 evaluation of the elbow point using the trajectory correlation coefficient as the performance metric. This elbow point
 52 serves as the threshold for identifying the target channels used in the inter-subject analysis. R, right lateral view; L,
 53 left lateral view.

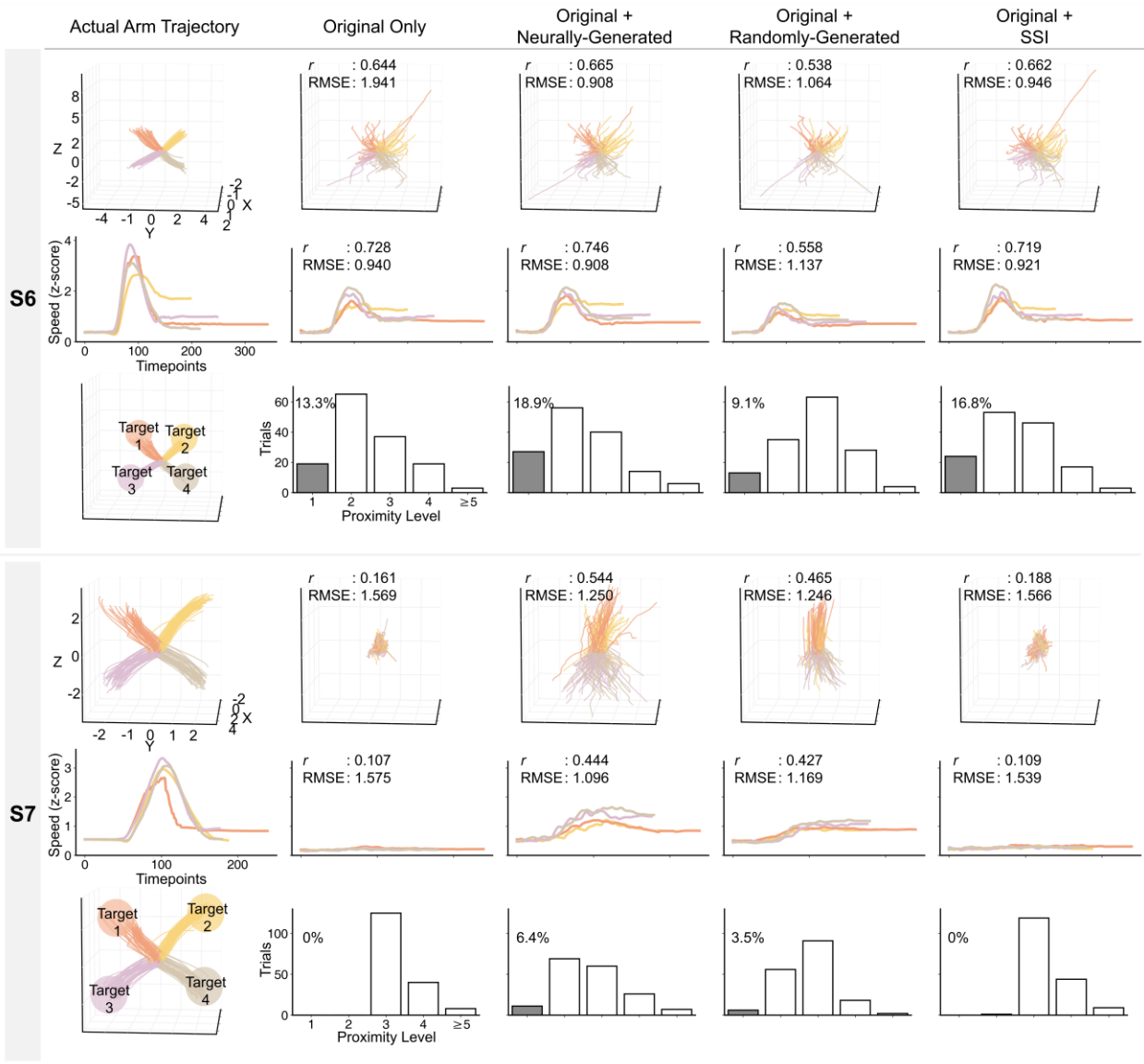


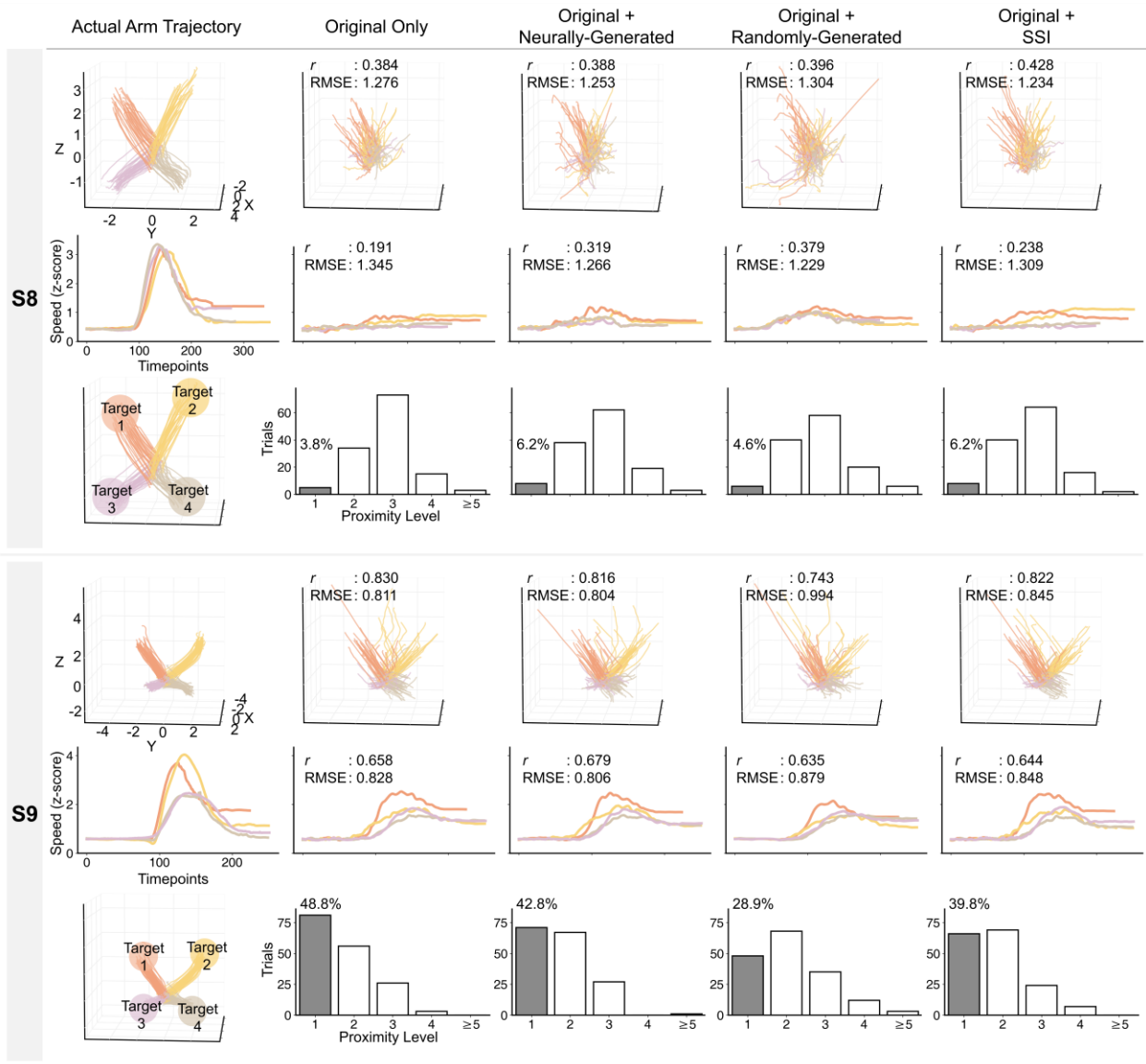
54

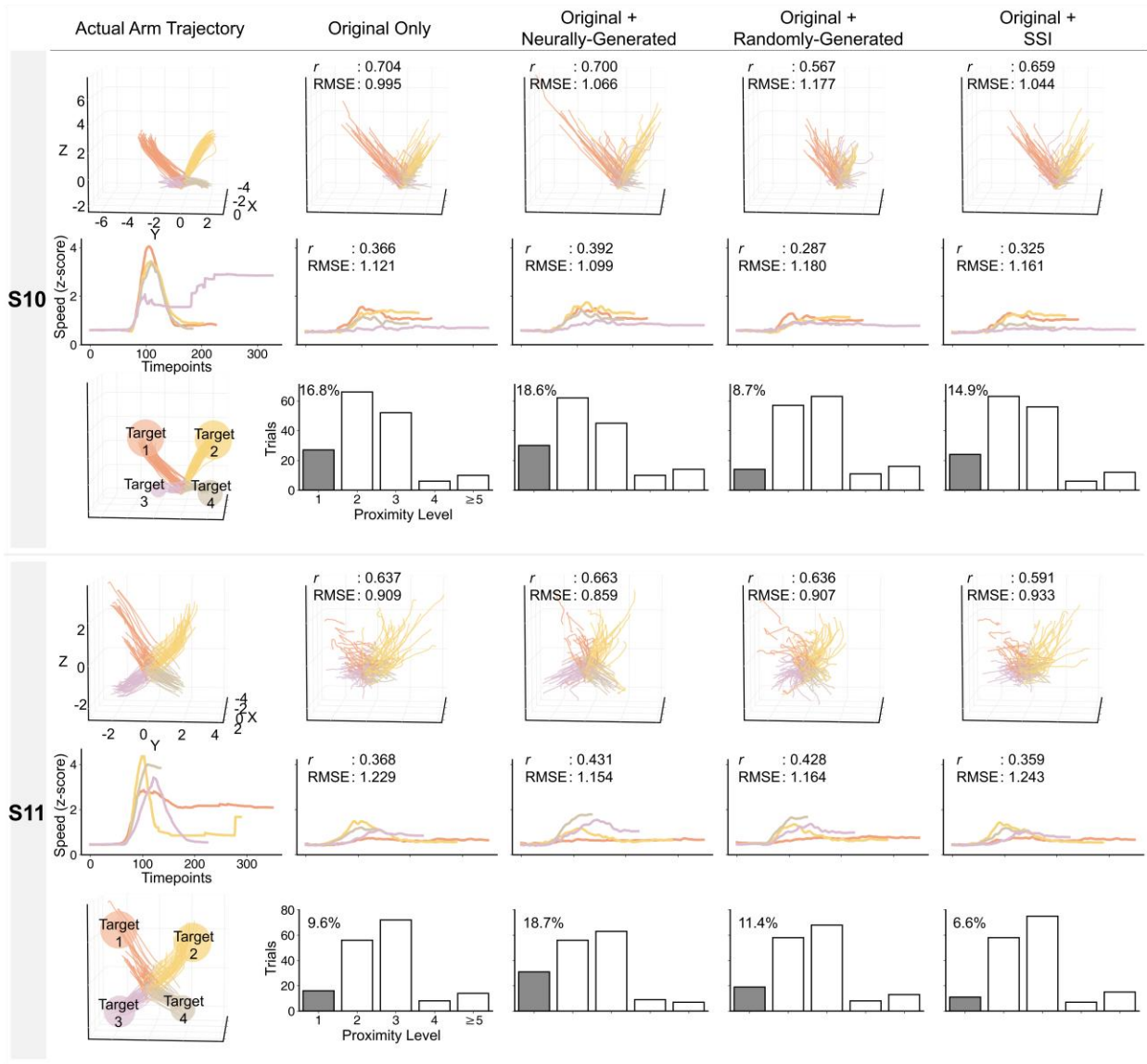
55 **Supplementary Figure 6. Spatial distribution of original and virtual electrodes.** Original channels are shown in
 56 black, and virtual channels are shown in pink ($n = 14$). R, right lateral view; L, left lateral view.

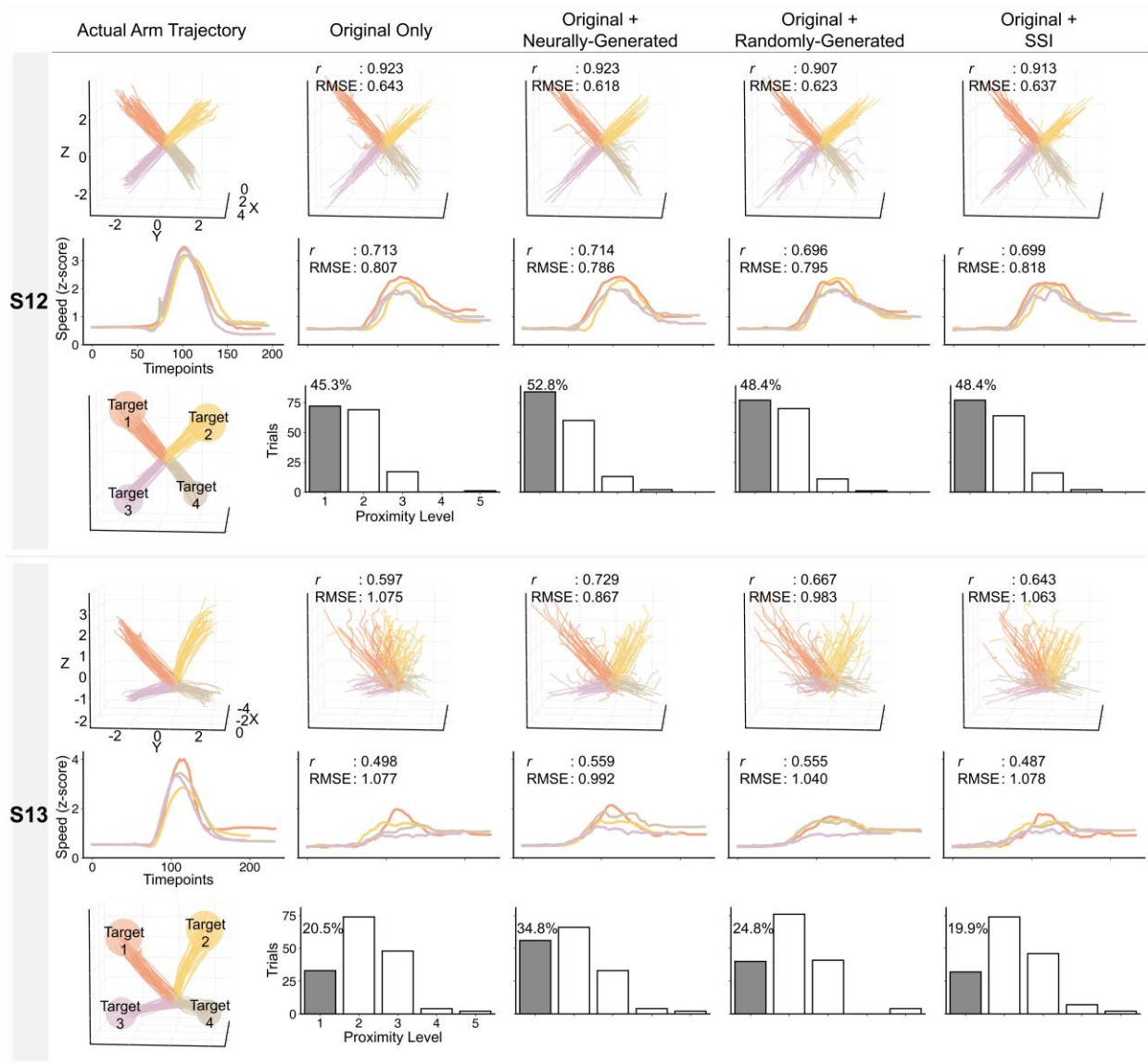


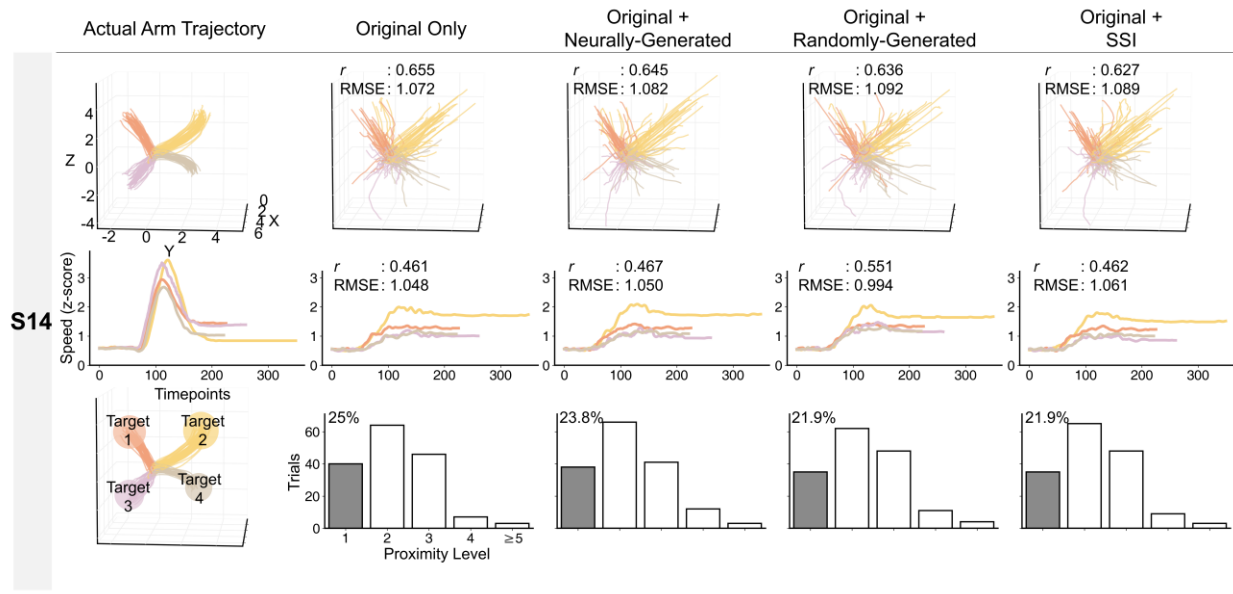






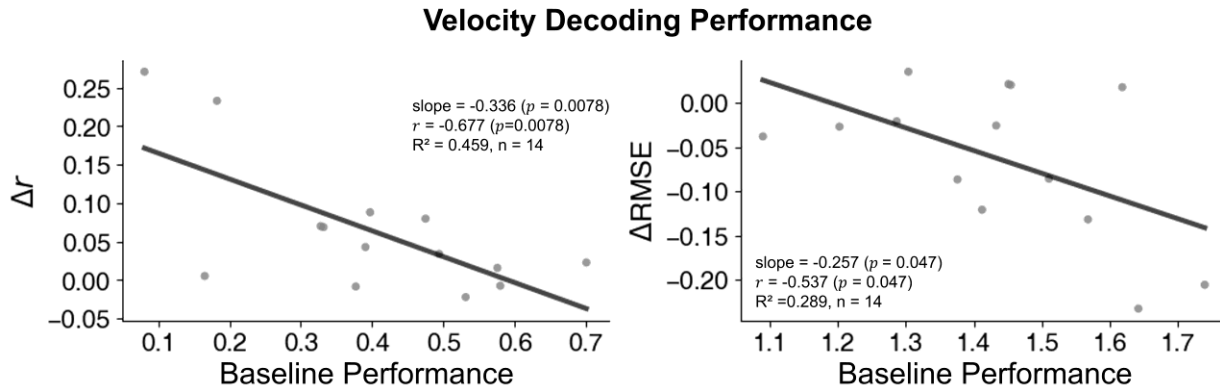






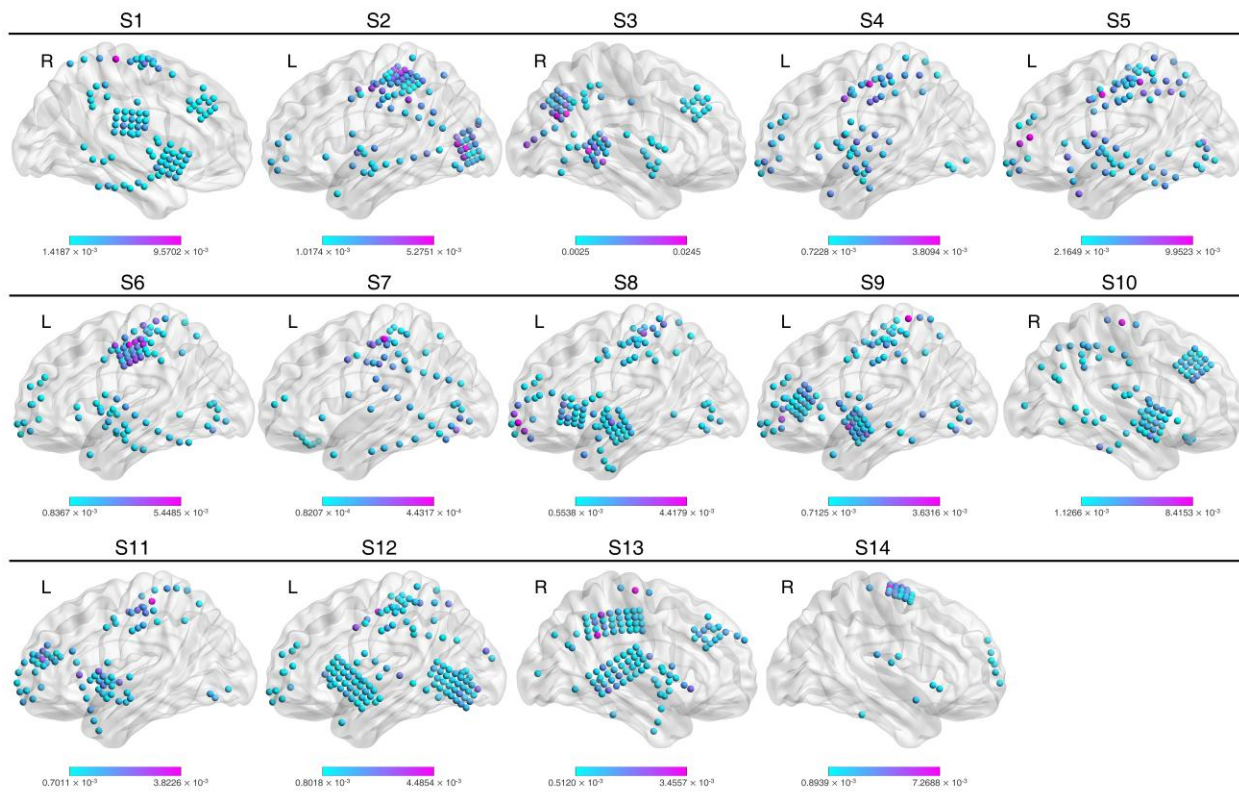
63

64 **Supplementary Figure 7. Inter-subject decoding results.** Inter-subject analysis results for individual subjects.
 65 Decoded trajectories, speed profiles, and endpoint reaching rate histograms are displayed, following the
 66 visualization format described in Figure 5.



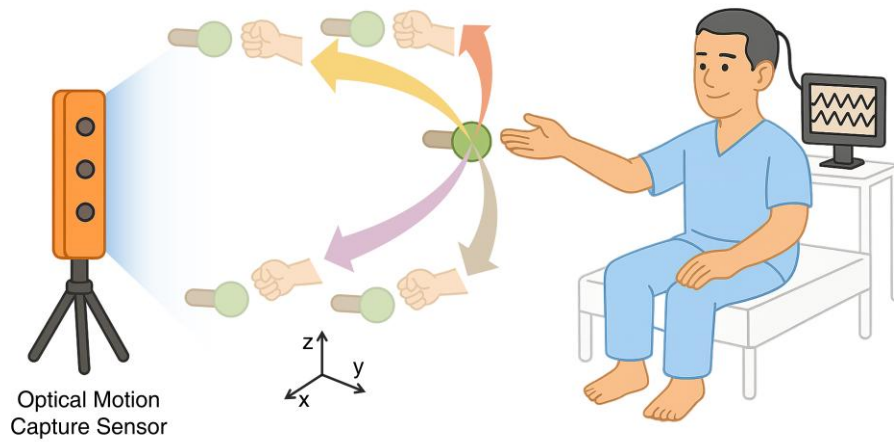
67

68 **Supplementary Figure 8. Greater decoding performance improvement in subjects with lower baseline**
 69 **performance.** Scatter plots show the relationship between original decoding performance and the improvement in
 70 velocity decoding performance, measured by Δr (left) and $\Delta RMSE$ (right). Δr and $\Delta RMSE$ were computed as the
 71 difference between decoding performance obtained with generated virtual channels and that obtained using
 72 implanted electrodes only. Linear regression analysis revealed a significant negative correlation in both metrics,
 73 indicating that subjects with lower baseline decoding performance exhibited greater performance improvements
 74 after incorporating virtual channels ($n = 14$).



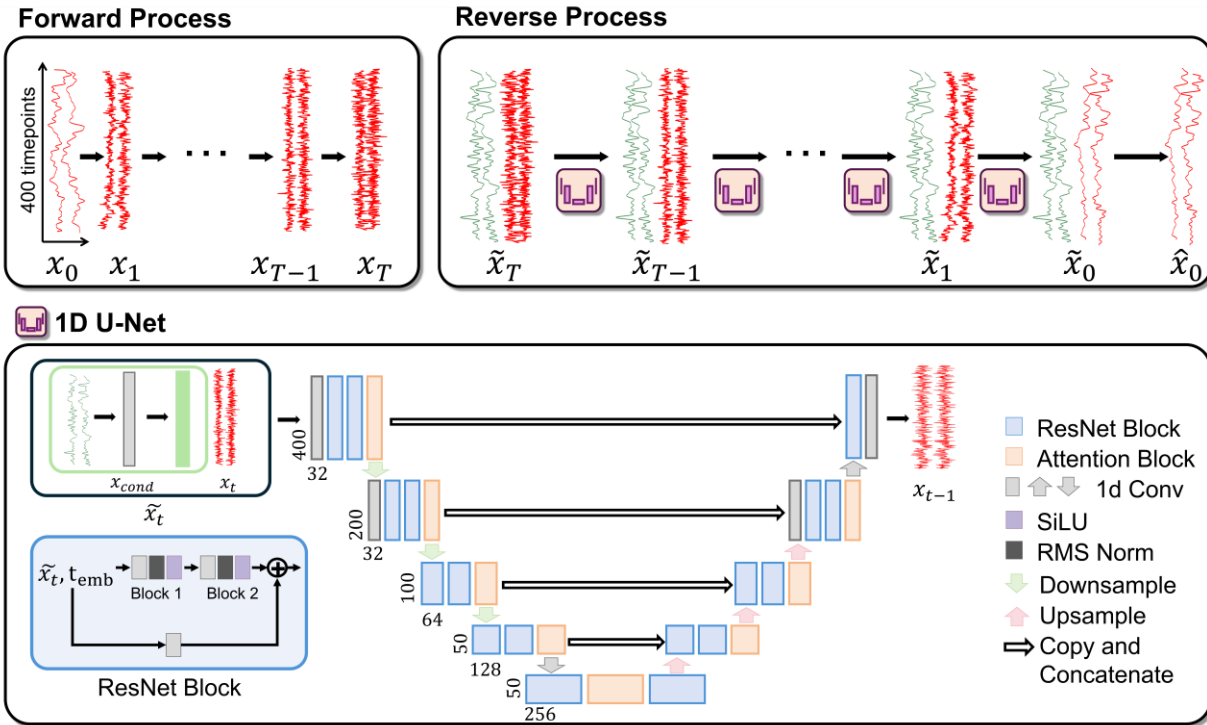
75

76 **Supplementary Figure 9. Inter-subject XAI contribution maps with generated virtual channels.** Explainable
 77 AI was applied to the decoder trained with generated virtual signals. Contribution maps include both implanted and
 78 generated virtual channels, color-coded by IG values, with higher values indicating greater contributions. R, right
 79 lateral view; L, left lateral view.



80

81 **Supplementary Figure 10. Experimental setup for center-out reach-and-grasp task.** Subjects performed the task
82 using the arm contralateral to the implanted hemisphere. Arm and hand movements were tracked at 100 Hz using an
83 optical motion capture sensor. The experimenter guided the target trajectories by manually moving a ball attached to
84 a rod toward one of four directions.



85

86 **Supplementary Figure 11. Overview of the DDPM Framework.** The top panel illustrates the mechanism of the
 87 diffusion process, consisting of forward and reverse processes. In the forward process, incremental noise is added
 88 to the original data (x_0) until it reaches a state of pure gaussian noise (x_T). In the Reverse Step, the U-Net architecture
 89 predicts the noise at each step to reconstruct the signal (\hat{x}_0) over 100 iterations ($T=100$). The bottom panel shows the
 90 detailed architecture of the 1D U-Net that executes reverse process. The U-Net is composed of 1-dimensional
 91 convolution (1d Conv), Residual Networks (ResNet), Sigmoid Linear Units (SiLU), Root Mean Square
 92 Normalization (RMS Norm) and Attention Block. To recognize the current diffusion stage, the model transforms the
 93 timestep t into a 32-dimensional embedding vector via sinusoidal embedding (t_{emb}), which is then expanded into
 94 128-dimensional temporal context through an multilayer perceptron (MLP). Within each ResNet block, this time
 95 embedding vector is further processed by an MLP and split into two values, scale and shift. These scale and shift
 96 values are directly applied to the \tilde{x}_t within the block to perform step-specific modulations.

97 **Supplementary Table 1. Intra-subject analysis cases.** This table summarizes the 110 generation cases used for the
98 intra-subject analysis. For each subject, every cortical region not containing a target channel was individually used
99 as a condition input. The table lists the corresponding AAL3 region numbers, with region names provided in
100 Supplementary Fig. 1. The number in parenthesis next to each region number indicates the number of implanted
101 electrodes within that region. The number of cases corresponds to the number of conditioning regions. Since five
102 target channels were selected per case, a total of 550 target-channel generations were produced across all subjects.

Subject	Target area	Condition area	Number of cases
	AAL3 region No. (number of electrodes)	AAL3 region No. (number of electrodes)	
S1	2 (2), 4 (2), 62 (7), 68 (8), 88 (9)	6 (1), 8 (3), 10 (1), 14 (3), 12 (2), 64 (1), 72 (1), 86 (6), 90 (3), 94 (5)	10
S2	55 (13), 57 (4), 61 (13)	1 (1), 47 (1), 49 (2), 53 (1), 65 (10), 67 (5), 69 (1), 89 (8)	8
S3	56 (11), 70 (9), 90 (15)	54 (2), 58 (1), 86 (4), 94 (1)	4
S5	5 (2), 11 (1), 61 (6), 65 (7), 91 (1)	1 (2), 9 (1), 13 (2), 67 (1), 69 (1), 85 (2), 87 (2), 89 (6), 93 (5)	9
S6	61 (17), 65 (3)	1 (2), 13 (1), 67 (3), 85 (2), 87 (1), 89(5), 93 (5)	7
S8	27 (1), 61 (3), 89 (16), 85 (4)	3 (3), 5 (1), 7 (3), 9 (11), 11 (7), 13 (1), 23 (1), 59 (1), 87 (1), 93 (2)	10
S9	1 (4), 85 (11), 89 (12)	3 (3), 5 (4), 9 (15), 11 (1), 13 (1), 61 (2), 63 (1), 71 (1), 93 (1)	9
S10	4 (5), 6 (13), 14 (4)	8 (1), 10 (2), 23 (1), 24 (1), 25 (1), 26 (1), 34 (2), 62 (1), 66 (3), 68 (1), 70 (1), 86 (8), 88 (5), 90 (3), 92 (1), 94 (2)	16
S11	1 (1), 3 (5), 5 (10), 7 (2), 71 (1)	9 (5), 11 (1), 13 (2), 21 (2), 23 (1), 61 (2), 63 (1), 85 (3), 87 (7), 91 (1), 93 (1)	11

S12	1 (2), 57 (10), 61 (5), 63 (3)	7 (5), 9 (8), 13 (2), 53 (2), 55 (3), 59 (1), 67 (2), 69 (2), 85 (7), 87 (5), 89 (22), 93 (4), 95 (1)	13
S13	66 (7), 68 (13), 86 (14), 90 (14)	2 (3), 4 (2), 6 (1), 8 (1), 14 (3), 20 (1), 62 (10), 70 (2), 88 (1), 94 (2)	10
S14	4 (16), 16 (3)	2 (2), 20 (3), 22 (1)	3
Total			110

103

104 **Supplementary Table 2. Inter-subject analysis channel configuration.** This table summarizes the train subjects
105 used and the number of channels before and after signal generation, including original channels, generated channels,
106 and the total number of channels used for decoding.

Subject	Number of original channels	Train Subjects	Number of generated virtual channels	Number of total channels
S1	54	S10, S13, S14	38	92
S2	59	S5, S6, S8, S9, S12	33	92
S3	43	S10, S13	33	76
S4	18	S5, S6, S8, S9, S11, S12	46	64
S5	39	S2, S6, S8, S9, S11, S12	45	84
S6	39	S2, S6, S8, S9, S11, S12	50	89
S7	26	S2, S5, S6, S12	33	59
S8	55	S2, S5, S6, S9, S11, S12	44	99
S9	56	S2, S5, S6, S8, S11, S12	46	102
S10	56	S1, S3, S13	26	82
S11	45	S5, S6, S8, S9, S12	33	78
S12	84	S2, S5, S6, S8, S9, S11	42	126
S13	74	S1, S3, S10	34	108

S14	25	S1	8	33
Total	673		511	1184

107

108 **Supplementary Table 3. Demographic and clinical characteristics of the subjects.** This table includes age, sex,

109 electrode hemisphere, total number of implanted electrodes, AAL3 region numbers and diagnosis of each subject.

110 The number in parentheses next to each AAL3 region number indicates the number of electrodes belonging to that

111 region.

Subject	Age	Sex	Electrode hemisphere	Number of electrodes	AAL3 region No. (number of electrodes)	Diagnosis
S1	22	F	Right	54	2 (2), 4 (2), 6 (1), 8 (3), 10 (1), 14 (3), 12 (2), 62 (7), 64 (1), 68 (8), 88 (9), 72 (1), 86 (6), 90 (3), 94 (5)	FLE
S2	24	M	Left	59	1 (1), 47 (1), 49 (2), 53 (1), 55 (13), 57 (4), 61 (13), 65 (10), 67 (5), 69 (1), 89 (8)	FLE
S3	28	M	Right	43	54 (2), 56 (11), 58 (1), 70 (9), 86 (4), 90 (15), 94 (1)	TLE
S4	27	F	Left	18	1 (1), 7 (1), 13 (1), 61 (5), 65 (2), 85 (4), 89 (3), 93 (1)	TLE
S5	36	F	Left	39	1 (2), 5 (2), 9 (1), 11 (1), 13 (2), 61 (6), 65 (7), 67 (1), 69 (1), 85 (2), 87 (2), 89 (6), 91 (1), 93 (5)	TLE
S6	58	M	Left	39	1 (2), 13 (1), 61 (17), 65 (3), 67 (3), 85 (2), 87 (1), 89(5), 93 (5)	TLE

S7	31	F	Left	26	23 (1), 24 (1), 25 (2), 26 (1), 27 (1), 55 (1), 57 (1), 61 (3), 67 (4), 69 (2), 85 (1), 89 (2), 93 (5), 95 (1)	TLE
S8	20	M	Left	55	3 (3), 5 (1), 7 (3), 9 (11), 11 (7), 13 (1), 23 (1), 27 (1), 59 (1), 61 (3), 85 (4) 87 (1), 89 (16), 93 (2)	FLE
S9	48	M	Left	56	1 (4), 3 (3), 5 (4), 9 (15), 11 (1), 13 (1), 61 (2), 63 (1), 71 (1), 85 (11), 89 (12), 93 (1)	TLE
S10	25	F	Right	56	4 (5), 6 (13), 8 (1), 10 (2), 14 (4), 23 (1), 24 (1), 25 (1), 26 (1), 34 (2), 62 (1), 66 (3), 68 (1), 70 (1), 86 (8), 88 (5), 90 (3), 92 (1), 94 (2)	TLE
S11	50	M	Left	45	1 (1), 3 (5), 5 (10), 7 (2), 9 (5), 11 (1), 13 (2), 21 (2), 23 (1), 61 (2), 63 (1), 71 (1), 85 (3), 87 (7), 91 (1), 93 (1)	FTLE
S12	18	F	Left	84	1 (2), 7 (5), 9 (8), 13 (2), 53 (2), 55 (3), 57 (10), 59 (1), 61 (5), 63 (3), 67 (2), 69 (2), 85 (7), 87 (5), 89 (22), 93 (4), 95 (1)	TLE
S13	23	M	Right	74	2 (3), 4 (2), 6 (1), 8 (1), 14 (3), 20 (1), 62 (10), 66 (7), 68 (13), 70 (2), 86 (14), 88 (1), 90 (14), 94 (2)	TLE
S14	21	M	Right	25	2 (2), 4 (16), 16 (3), 20 (3), 22 (1)	FLE

112 FLE, frontal lobe epilepsy; TLE, temporal lobe epilepsy; FTLE; frontal and temporal lobe epilepsy.

113 **Supplementary Table 4. Number of trials per session for each participant.** Values separated by commas indicate
 114 the number of trials in session 1 and session 2, respectively. Bad trials were excluded. Columns labeled Direction 1-
 115 4 correspond to the number of trials performed toward each of the four target directions in the center-out reach-and-
 116 grasp task.

Subject	Number of trials (Session 1, 2)	Direction 1	Direction 2	Direction 3	Direction 4
S1	60, 73	18, 23	11, 13	16, 19	15, 18
S2	80, 92	24, 27	16, 19	21, 23	19, 23
S3	75, 81	24, 24	13, 16	18, 20	20, 21
S4	53, 23	16, 7	10, 5	15, 5	12, 6
S5	77, 39	25, 13	12, 7	19, 11	21, 8
S6	79, 64	24, 20	16, 13	20, 16	19, 15
S7	81, 92	20, 23	20, 23	21, 22	20, 24
S8	76, 54	20, 14	17, 14	20, 13	19, 13
S9	81, 85	20, 21	20, 21	24, 21	17, 22
S10	79, 82	20, 21	20, 20	20, 20	19, 21
S11	82, 84	20, 21	20, 21	23, 22	19, 20
S12	80, 79	20, 19	20, 20	20, 20	20, 20
S13	76, 85	19, 21	20, 21	18, 22	19, 21
S14	80, 80	20, 20	20, 20	20, 20	20, 20

118 **Supplementary Table 5. Model architecture of the Bi-LSTM decoder.** The decoder consisted of two Bi-LSTM
 119 layers followed by dropout and two linear layers. The table provides a representative example from Subject S1 with
 120 54 input electrodes; the same architecture was applied across all subjects.

Layer name (activation)	Number of trainable parameters	Output shape	Note
Input Sequence	-	[Batch, 10, 54]	Batch size, sequence length = 10, number of electrodes = 54
bLSTM (tanh)	22,528	[Batch, 10, 64]	First Bi-LSTM layer
Dropout	-	[Batch, 10, 64]	Dropout rate = 0.1
bLSTM (tanh)	10,496	[Batch, 10, 32]	Second Bi-LSTM layer
Dropout	-	[Batch, 10, 32]	Dropout rate = 0.1
Linear (ReLU)	2,112	[Batch, 64]	Fully connected layer
Dropout	-	[Batch, 64]	Dropout rate = 0.1
Linear (linear)	195	[Batch, 3]	Output layer predicting 3- axis hand velocity
Total number of trainable parameters	35,331	-	-